Catalytic behavior of alumina-promoted sulfated zirconia supported on mesoporous silica in butane isomerization

Chang-Lin Chen [a,b], Tao Li [a], Soofin Cheng [a], Nanping Xu [b], and Chung-Yuan Mou [a,*]

[a] *Department of Chemistry, National Taiwan University, Taipei, Taiwan 106, P.R. China*
[b] *College of Chemical Engineering, Nanjing University of Technology, Nanjing, China 210009*

Received 10 July 2001; revised 11 October 2001; accepted 16 October 2001

Alumina-promoted sulfated zirconia was supported on mesoporous molecular sieves of pure-silica MCM-41 and SBA-15. The catalysts were prepared by "direct impregnation" of metal sulfate onto the as-synthesized MCM-41 and SBA-15 materials, followed by solid state dispersion and thermal decomposition. Measurements of XRD and nitrogen adsorption isotherms showed that the structures of resultant materials retain well-ordered pores, even with ZrO_2 loading as high as 50 wt%. The characterization results indicated that most of the promoted sulfated zirconia were well dispersed on the internal surface of the ordered mesopores. The catalytic behavior of the alumina-promoted sulfated zirconia supported on mesoporous silica was studied in *n*-butane isomerization. The supports of mesoporous structures led to high dispersion of sulfated zirconia in the meta-stable tetragonal phase, which was the catalytic active phase. The high performance of alumina-promoted catalysts was ascribed to the sulfur retention by alumina.

KEY WORDS: sulfated zirconia; mesoporous silica; MCM-41; SBA-15; isomerization of butane; alumina.

1. Introduction

Sulfated zirconia (abbreviated as S-ZrO_2) has attracted intensive attention in the past two decades because it is considered as an environmentally friendly strong solid acid and it has high catalytic activity in the isomerization of alkanes at relatively low temperatures. Recent studies in the preparation and applications of sulfated zirconia have been reviewed in several articles [1–3]. Among the various factors which may affect the catalytic activity, surface area of the original ZrO_2 was considered to be important [4]. However, it is difficult to increase the surface area of zirconia by conventional preparation methods. To overcome this problem, some researchers engaged in supporting S-ZrO_2 on porous materials with high surface area, such as SiO_2 and Al_2O_3 [5–8]. Silica-based mesoporous materials, such as MCM-41 [9] and SBA-15 [10], are potential catalyst supports because of their high thermal stability (up to 800 °C), large surface area (above 1000 m^2/g), uniform-sized pores and relatively small diffusion hindrance, which facilitates the diffusion of molecules in and out of the mesopores [11–14].

A few papers have recently reported on the preparation of supported S-ZrO_2 on MCM-41, SBA-15 [15,16] and FSM-16 [17]. They were prepared by a two-step impregnation method. The ZrO_2 was loaded on calcined mesoporous materials either by an impregnation method [15,17] or by chemical liquid deposition [16], then it was sulfated with sulfuric acid, followed by calcination. We recently reported on the preparation of S-ZrO_2/MCM-41 by the incipient wetness impregnation method started with calcined MCM-41 and zirconium sulfate [18,19]. The spreading is followed by calcinations. Although strong acidity was observed in butane isomerization, the porous structure of MCM-41 could be seriously blocked when the ZrO_2 loading was high. A similar preparation method was also adopted by Wang and Guin [20], but the materials were not well characterized.

Very recently, we succeeded in very high loading of S-ZrO_2 (~60%) onto as-synthesized MCM-41 [21]. The un-removed surfactants serve as a scaffold in stabilizing the mesostructure of S-ZrO_2/MCM-41 during direct impregnation. Isomerization of butane was the test reaction for catalysis. In this paper, we continue this study while focusing on the effect of aluminum promotion in the catalysis. Gao *et al.* [22,23], Canton *et al.* [24] and we [19] have previously reported that addition of a proper amount of alumina into S-ZrO_2 improves its catalytic performance. The cause of the promotion effect is still not clear.

2. Experimental

2.1. Sample preparation

As-synthesized pure siliceous MCM-41 was prepared using the delayed neutralization processes reported by Lin *et al.* [25]. The molar composition of the gel is 1.0 CTMABr : 2.0 SiO_2 : 0.8 Na_2O : 0.67 H_2SO_4 : 1.0 acetone : 133 H_2O. The gel was crystallized in static condition

* To whom correspondence should be addressed.
E-mail: cymou@ccms.ntu.edu.tw

1011-372X/02/0300-0223/0

at 100 °C for 5 days. Then the solid product was filtered, washed with deionized water, and dried in air at room temperature.

As-synthesized pure siliceous SBA-15 was prepared according to the procedures reported by Zhao *et al.* [10] In a typical synthesis, 1 g of amphiphilic triblock copolymer, poly(ethylene glycol)-poly(propylene glycol)-poly(ethylene glycol) (average MW 5800), was dispersed with stirring in a solution of 30 g water and 9.5 g 35% HCl, followed by addition of 2.3 g of tetraethyl orthosilicate and continuous stirring at 40 °C for 24 h. Then the solid product was filtered, washed and dried in air at room temperature.

Alumina-promoted S-ZrO_2 supported on MCM-41, SBA-15 and a commercial silica were prepared in a similar way as that reported in our previous paper [21]. They are designated as SZA/MCM-41, SZA/SBA-15 and SZA/SiO_2, respectively. The as-synthesized mesoporous materials or commercial silica in powder form were suspended in a methanol solution of zirconium sulfate and aluminum sulfate and stirred at 50 °C for about 30 min, then dried at 110 °C to remove the solvent. The solid was heated at 400 °C in static air to decompose the remaining template and solid-state dispersion of zirconium/aluminum sulfates. Finally, the solid was heated at 720 °C for 3 h to decompose the sulfates. In order to examine the effect of alumina, ZrO_2 content was kept at 50 wt% on each support, which is close to the dispersion threshold of zirconia sulfate on MCM-41.

2.2. Characterization

X-ray powder diffraction patterns of the samples were obtained on a Scintag X1 diffractometer using monochromatic Cu Kα radiation ($\lambda = 0.154$ nm) at 40 kV and 30 mA. Surface areas and N_2 adsorption–desorption isotherms were measured with a Micromeritics ASAP 2000 automatic adsorption instrument. Solid-state ^{27}Al MAS-NMR spectra were taken on a Bruker DSX400 WB NMR spectrometer. Sulfur and aluminum contents in the calcined catalysts were determined by inductively coupled plasma atomic emission spectrometry (ICP-AES) using a Jarrel-Ash ICAP 9000 instrument with HF-dissolved samples.

2.3. Catalytic experiments

The supported S-ZrO_2 samples were tested as catalysts in *n*-butane isomerization using a fixed-bed continuous flow reactor. The reactor was operated at atmospheric pressure. Approximately 1.0 g of the catalyst was loaded into the reactor and then pretreated in flowing dry air (60 ml min^{-1}) at 450 °C for 3 h. The reactor temperature was then lowered to the reaction temperature of 250 °C or other desired temperature. The feed gas *n*-butane/H_2 mixtures (1:10 v/v) flowed through the catalyst bed at an *n*-butane weight hourly space velocity (WHSV) of 0.3 h^{-1}. An on-line Shimadzu 14B gas chromatograph equipped with FID was used to analyze the reaction products.

3. Results and discussion

3.1 Characterization

Figure 1 shows the XRD patterns of the SZA/MCM-41 composites with 50 wt% ZrO_2 and 2.2 wt% Al_2O_3 after calcination at various temperatures for 3 h. All the patterns show the typical diffraction peaks of MCM-41 in the low 2θ region. This indicates that the regular arrangement of mesoporous structure is preserved on SZA/MCM-41. In the high 2θ region, the XRD patterns show broad peaks at $2\theta = 30.3$, 35.0, 50.4, 60.2 and 63.0 °, indicating the presence of tetragonal ZrO_2 nanocrystalline phase. We note that the step of solids being pre-heated at 400 °C in static air for dispersion of zirconium/aluminum sulfates is very important. It helps the formation of the nanophase. The meta-stable tetragonal ZrO_2 is believed to be the phase for high catalytic activity of S-ZrO_2. Although the cubic ZrO_2 has a similar XRD pattern as the tetragonal phase, the presence of a cubic phase is not considered because it is a high temperature phase and easily transformed to tetragonal phase in the temperature range under investigation [26]. At the calcination temperature of 650–700 °C, the intensity of the diffraction peaks of tetragonal ZrO_2 was found to increase with calcination temperature. Further increasing the calcination temperature up to 740 °C, the intensity of these peaks remains almost unchanged.

According to the TG analysis (figure 2), most of the $Zr(SO_4)_2$ decomposes around 650–700 °C following the reaction $Zr(SO_4)_2 \rightarrow ZrO_2 + 2SO_3$. However, a small portion of the sulfates should remain on the zirconia surface to form the active sulfated zirconia phase. The sulfur contents of the calcined samples are shown in

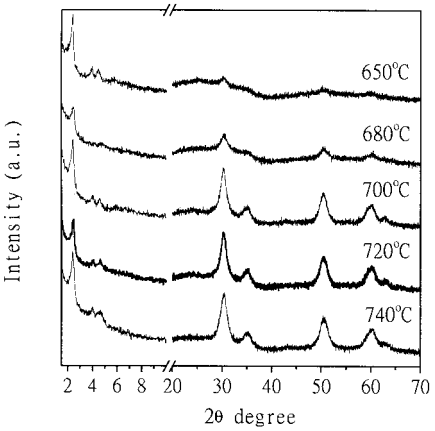

Figure 1. XRD patterns of the composites of SZA/MCM-41 with 50 wt% ZrO_2 and 2.2 wt% Al_2O_3 calcined at various temperature for 3 h in air.

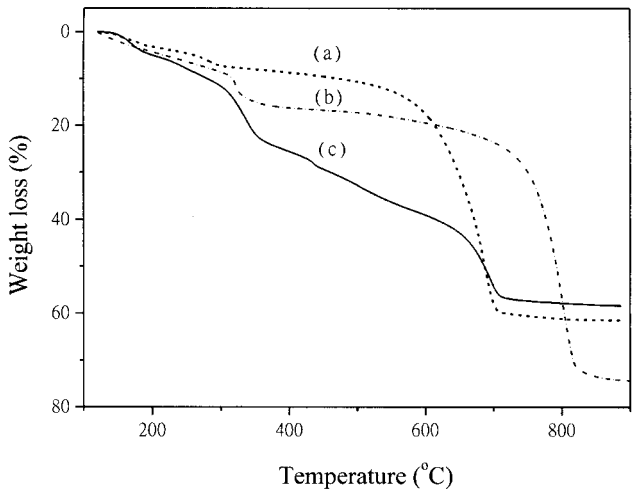

Figure 2. TG analysis of (a) $Zr(SO_4)_2$, (b) $Al_2(SO_4)_3$ and (c) the precursor of SZA/MCM-41 with 50 wt% ZrO_2 and 2.2 wt% Al_2O_3.

table 1. The value was found to decrease as the calcination temperature increased. These results are reasonable because more SO_3 should be released when the sample is heated at higher temperature. On the other hand, it is noticeable that the sulfur content increases with the Al_2O_3 content. TG analysis shows that complete decomposition of aluminum sulfate occurs at relatively higher temperature, *ca.* 800 °C. Therefore, Al_2O_3 probably plays an important role in preserving sulfate on the catalyst surface.

Table 1 also shows the surface areas and pore volumes of the samples. Over the MCM-41 support, all the samples have relatively high surface area, around 500 m^2/g. It is noticed that the Al_2O_3 content has little effect on the surface area and pore volume, while calcination temperature affects the surface area markedly. For SZA/MCM-41 containing 50% ZrO_2 and 2.2% Al_2O_3, the surface area increases from 415 m^2/g upon 650 °C calcination to 512 m^2/g at 700 °C. When the calcination temperature is

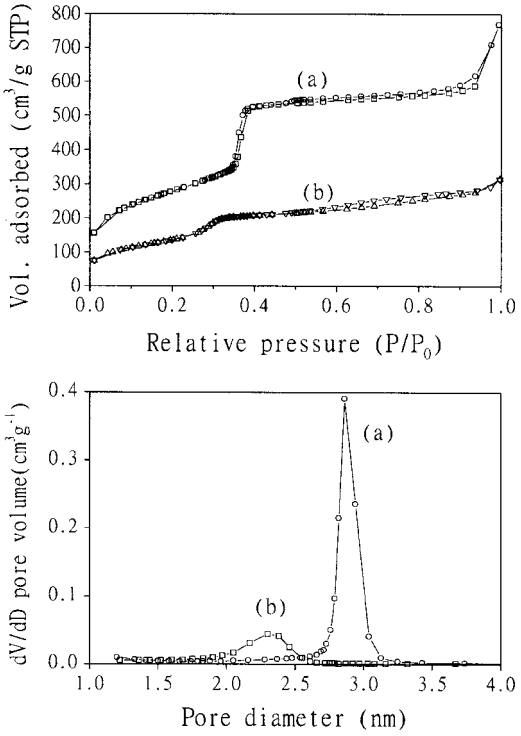

Figure 3. N_2 adsorption–desorption isotherms and pore size distribution curves of (a) MCM-41 and (b) calcined SZA/MCM-41 with 50 wt% ZrO_2 and 2.2 wt% Al_2O_3.

further raised up to 740 °C, the surface area decreases slightly to 493 m^2/g. This phenomenon can be explained in connection with the change in XRD patterns of SZA/MCM-41 calcined at various temperatures. The increase in surface area is due to the decomposition of zirconium sulfate occluded in the mesopores to form sulfated zirconia. As the calcination temperature further increases to 700–740 °C, zirconia probably sinters to form larger crystallites and a portion of them blocks the pores.

Figure 3 shows the N_2 adsorption–desorption isotherm and pore size distribution of SZA/MCM-41 in

Table 1
Physico-chemical properties of the supported catalysts and the supports

Sample code	Calc. temperature (°C)	Al_2O_3 content (wt%)	Sulfur content (wt%)	BET S.A. (m^2/g)	Pore volume (ml/g)
[a] SZ/MCM-41	720	0.0	0.51	488	0.47
[a] SZA/MCM-41	720	1.3	1.07	492	0.46
[a] SZA/MCM-41	720	2.2	1.42	497	0.48
[a] SZA/MCM-41	720	3.1	1.94	509	0.46
[a] SZA/MCM-41	650	2.2	2.27	415	0.39
[a] SZA/MCM-41	680	2.2	1.81	446	0.41
[a] SZA/MCM-41	700	2.2	1.61	512	0.51
[a] SZA/MCM-41	740	2.2	0.91	493	0.44
[a] SZA/SBA-15	720	2.2	3.01	178	0.25
[a] SZA/SiO_2	720	2.2	1.41	250	0.39
MCM-41	680	—	—	1010	1.10
SBA-15	680	—	—	880	0.92
SiO_2	—	—	—	525	—

[a] Samples contain 50 wt% ZrO_2.

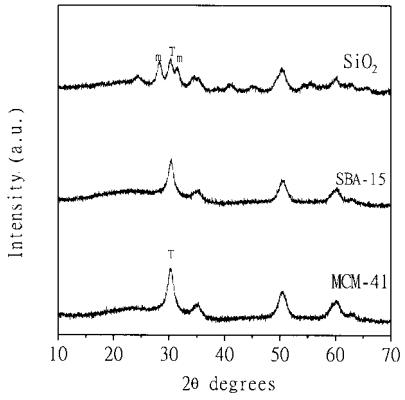

Figure 4. XRD patterns of SZA with 50 wt% ZrO_2 and 2.2 wt% Al_2O_3 supported on different carriers calcined at 720 °C for 3 h in air [m: monoclinic zirconia; T: tetragonal zirconia].

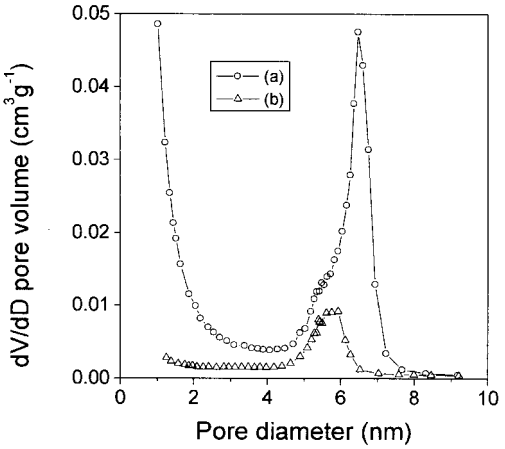

Figure 5. Effect of final calcination temperature on the surface area and pore volume of SZA/MCM-41 with 50 wt% ZrO_2 and 2.2 wt% Al_2O_3.

comparison to those of pristine MCM-41. The isotherm for calcined MCM-41 has a type IV shape. Upon supporting S-ZrO_2 on MCM-41 to form SZA/MCM-41, the N_2 adsorption amount decreases and the capillary condensation profile becomes flatter. Concomitantly, the maximum pore diameter of MCM-41 decreased from 2.9 nm to 2.2 nm when S-ZrO_2 was introduced. These results show that the S-ZrO_2 should be dispersed on the inner surface of the mesopores and alters the diameter and shape of the pores.

Figure 4 shows the XRD patterns of S-ZrO_2 supported on different carriers. With MCM-41 and SBA-15 as the supports, only the meta-stable tetragonal ZrO_2 phase was observed. But on the silica support, the diffraction lines of both tetragonal and monoclinic zirconia phases can be seen. Xie *et al.* [7] studied the dispersion of zirconium sulfate on silica. They reported that the apparent dispersion threshold of zirconium sulfate is *ca.* 0.26 g/100 m^2 on a silica surface. Below or close to the apparent dispersion threshold, the decomposed zirconium sulfate always forms tetragonal zirconia. However, if the zirconium sulfate loading is greater than the apparent dispersion threshold, it decomposes to form predominantly monoclinic zirconia. Garvie [26] studied the formation of tetragonal ZrO_2 phase as a function of crystallite size. He proposed that 30 nm was the critical crystallite size for meta-stable tetragonal ZrO_2 to present at ambient temperature. Above this size, tetragonal ZrO_2 could not exist at room temperature and would transform to monoclinic phase. Accordingly, the apparent dispersion threshold is likely the critical loading of ZrO_2 on the support to form ZrO_2 crystallites of less than 30 nm. The surface areas of pristine MCM-41, SBA-15 and the commercial silica in this work are 1010, 880 and 500 m^2/g, respectively. If 50 wt% ZrO_2 on MCM-41 and SBA-15 is close to the apparent dispersion threshold, that amount should be greater than the apparent dispersion threshold for commercial silica. It has been reported that sulfated ZrO_2 of meta-stable tetragonal phase has higher catalytic activity than the monoclinic phase [27,28]. From this point of view, sulfated zirconia supported on mesoporous materials should have higher catalytic activity. That was confirmed by a later isomerization reaction test.

Table 1 shows that SBA-15 and silica gel loaded with the same amount of ZrO_2 as MCM-41 have much lower surface areas of 178 and 250 m^2/g, respectively. The reason for the low surface area of SZA/SBA-15 is that there are a lot of micropores on the wall of SBA-15 as reported recently [29,30]. In this work, the size of the micropore is less than 1.5 nm. The presence of micropores in pristine SBA-15 is shown in figure 5. After supporting S-ZrO_2 on SBA-15, the micropores disappeared (also shown in figure 5). S-ZrO_2 was considered to fill the micropores on SBA-15. As a result, the surface area of SZA/SBA-15 reduces significantly in comparison to that of SZA/MCM-41. Although the surface area of SZA/SBA-15 is low, the sulfur content in SZA/SBA-15 is relatively high. The reaction test also shows that it has good catalytic performance in *n*-butane isomerization. The high sulfur content is attributed to the trapping of sulfate species inside the micropores of SBA-15, and they are not as easily decomposed as those in the mesopores.

^{27}Al MAS NMR is a most revealing method for examining the coordination state of aluminum. Figure 6 shows the ^{27}Al MAS NMR spectra of alumina-promoted sulfated zirconia supported on three different supports: MCM-41, SBA-15 and silica gel. Only a sharp peak at *ca.* 0 ppm, corresponding to Al in octahedral coordination, was observed. No peak at about 50 ppm, corresponding to tetrahedrally coordinated Al, can be seen in either sample. These results indicate that all the Al atoms are probably in the oxide forms and situated in extra-framework of the supports.

3.2. *Catalytic activity in* n-*butane isomerization*

The effect of alumina content on the catalytic activity of SZA/MCM-41 in isomerization of *n*-butane

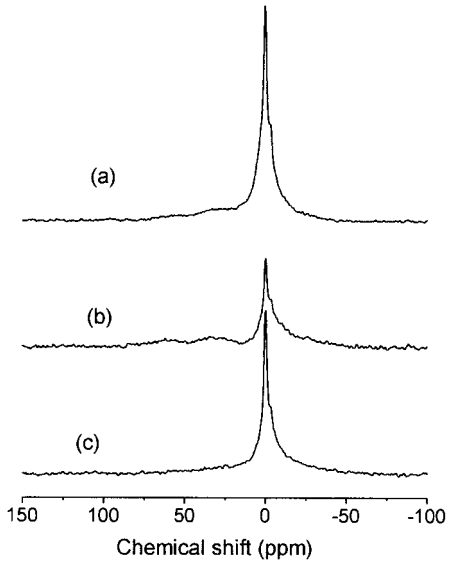

Figure 6. ^{27}Al MAS NMR spectra of (a) SZA/SiO_2; (b) SZA/MCM-41; (c) SZA/SBA-15.

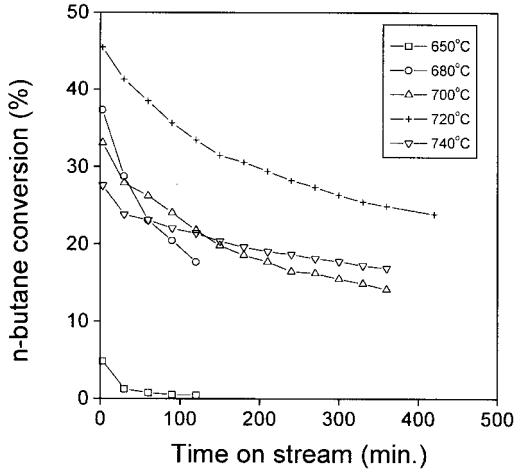

Figure 8. The effect of final calcination temperature on the catalytic activity over SZA/MCM-41 with 50 wt% ZrO_2 and 2.2 wt% Al_2O_3.

to *iso*-butane was studied. The selectivity to *iso*-butane was higher than 95%, and only minor amounts of methane, propane and pentane were formed. The variation of the conversion versus time on stream over SZA/MCM-41 with different alumina contents is given in figure 7. The activity of the sample without alumina was much lower. The addition of a small amount of alumina can greatly improve the catalytic activity. The optimal activity was observed when the alumina content reached about 2.2 wt% in the sample. Further increasing the alumina loading decreased the catalytic activity. All these MCM-41 supported catalysts have zirconia in the meta-stable tetragonal phase, and the sulfur content increases with alumina content. The appearance of an optimal alumina loading on the catalytic activity implies that an excess amount of alumina may cover the zirconia surface and reduce the catalytically active sites. On the other hand, although the catalytic activity decays gradually with time on stream, the activity can be completely restored by thermal treatment in air at 450 °C [31].

Figure 8 shows the effect of final calcination temperature on the catalytic activity. The catalytic activity of the samples increased with the final calcination temperature. This is attributed to the fact that the amount of catalytically active tetragonal ZrO_2 phase increases with the final calcination temperature. The optimal activity was obtained when the SZA/MCM-41 sample was calcined at about 720 °C. Since the sulfur content decreases as the calcination temperature increases, the 720 °C calcination temperature for optimal catalytic activity is probably a compromise between the sulfur content and the amount of tetragonal ZrO_2 phase.

The variation of the conversion versus time on stream for SZA/MCM-41 with different reaction temperature is given in figure 9. It was observed that higher reaction temperature gave higher initial activity, which was, however, followed by rapid decay. If the reaction was run at a

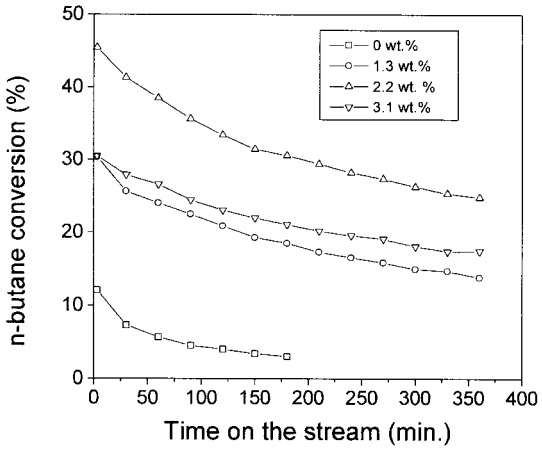

Figure 7. Conversions of *n*-butane *versus* time on stream over SZA/MCM-41 with 50 wt% of ZrO_2 and different amount of Al_2O_3.

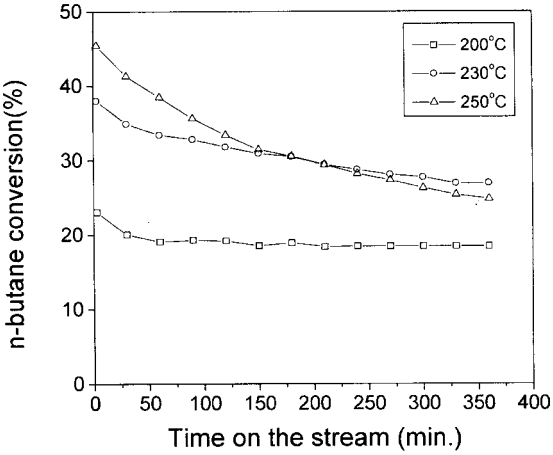

Figure 9. The effect of reaction temperature on *n*-butane conversion *versus* time on stream over SZA/MCM-41 with 50 wt% ZrO_2 and 2.2 wt% Al_2O_3.

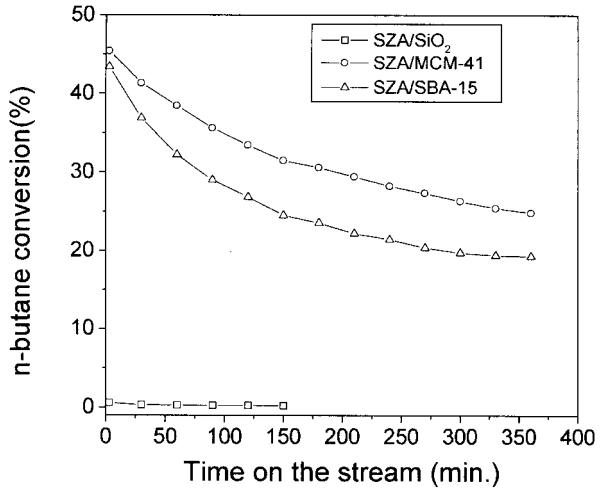

Figure 10. The comparison of catalytic activity of *n*-butane isomerization *versus* time on stream over SZA with 50 wt% ZrO_2 and 2.2 wt% Al_2O_3 supported on different carriers calcined at 720 °C for 3 h in air.

lower temperature of 200 °C, though the initial activity was lower the activity became more stable over the time on stream.

Figure 10 compares the catalytic activities of alumina-promoted S-ZrO_2 supported on three different supports in *n*-butane isomerization. Both SZA/MCM-41 and SZA/SBA-15 have ordered mesopores and narrow pore size distribution, while SZA/SiO_2 has irregular pore size distribution. These three catalysts were prepared in the same way and have the same Al and ZrO_2 content. The results showed that similar trends were observed over SZA/MCM-41 and SZA/SBA-15, while SZA/SiO_2 gave only trace activity. It is noticeable that although SZA/SBA-15 has the lowest surface area of 178 m^2/g, it has much higher catalytic activity than SZA/SiO_2 (249 m^2/g). On the other hand, SZA/MCM-41 which has a surface area of 497 m^2/g (three times that of SZA/SBA-15) is just slightly more active than SZA/SBA-15. It is obvious that the catalytic performance cannot be interpreted simply by surface area. The crystalline form of ZrO_2 plays a very important role in catalytic activity. The low catalytic activity of SZA/SiO_2 is likely due to the fact that ZrO_2 is present in both tetragonal and monoclinic phases. On mesoporous MCM-41 and SBA-15 materials, the large surface area and mesoporous structures would help better dispersion of sulfated ZrO_2 and restrict the ZrO_2 crystallite size. That consequently prevents the transformation of tetragonal zirconia into monoclinic zirconia. Therefore, the mesoporosity is crucial in determining the structure and activity of the catalyst. The promoter effect of alumina is mostly due to sulfur retention. Previously, Canton *et al.* had associated the increased catalytic activity in Al-promoted SZ with the decrease in particle size of ZrO_2 [24]. Here we also reach the high dispersions of zirconia by using the nanochannels of MCM-41 as confined space. Finally, we note that Gao *et al.* [23] had attributed the promotional effect of alumina to the increased acid sites of medium strength. From our point of view, this is expected since increased surface area and sulfation would increase surface acidic sites.

4. Conclusions

Alumina-promoted sulfated zirconia was successfully supported on all-silica mesoporous MCM-41 and SBA-15 by "direct method of impregnation" followed by solid-state dispersion and decomposition of the corresponding metal sulfate.

Ordered mesoporous materials with large surface area are beneficial towards supporting a large amount of zirconium sulfate and its decomposition in forming tetragonal sulfated zirconia, which is the catalytically active phase in hydrocarbon isomerization. The adsorption–desorption analyses indicated that most of the catalytically active phases were on the internal surface of the mesoporous materials.

The addition of a small amount of alumina enhances the catalytic activity for *n*-butane conversion. This may be due to the retention of a higher amount of sulfur species on the surface of catalysts.

The catalytic studies in isomerization of *n*-butane show that the activity is strongly dependent on the final calcination temperature. The optimal calcination temperature is about 720 °C. The reaction temperature has a great influence on the reaction behavior. There is an optimum reaction temperature of 230 °C. However, we also found that lower reaction temperature would slow down the decay of the catalytic activity.

Both SZA/MCM-41 and SZA/SBA-15 have much higher catalytic activity in comparison with SZA/SiO_2. The main reason is that mesoporous carriers can help better dispersion of sulfated tetragonal ZrO_2 and prevent the transformation of tetragonal sulfated zirconia into monoclinic sulfated zirconia.

Acknowledgments

We gratefully acknowledge the financial support from the Ministry of Education of Taiwan. C.-L. Chen thanks the financial support given by the Education Commission of Jianshu Province, China (Project 00KJB530001). We also thank Ms. M.C. Chao for the synthesis of SBA-15, Drs. H.-P. Lin and S.-T. Wong for helpful discussions, and Dr. Zhao Qi for his help in NMR experiments.

References

[1] X.M. Song and A. Sayari, Catal. Rev.-Sci. Eng. 38 (1996) 329.
[2] V. Adeeva, H.Y. Liu, B.Q. Xu and W.M.H. Sachtler, Top. Catal. 6 (1998) 61.

[3] G.D. Yadav and J.J. Nair, Microporous Mesoporous Mater. 33 (1999) 1.
[4] A. Corma, M.I. Juan-Rajadell and J.M. Lopez Nieto, Appl. Catal. A. 116 (1994) 151.
[5] T. Ishida, T. Yamaguchi and K. Tanabe, Chem. Lett. (1998) 1869.
[6] J.M. Grau, C.R. Vera and J.M. Parera., Appl. Catal. A.172 (1998) 311.
[7] Y.-Y. Huang, B.-Y. Zhao and Y.-C. Xie, Appl. Catal. A. 173 (1998) 27.
[8] T. Lei, J.S. Xu, Y. Tang, W.-M. Hua and Z. Gao, Appl. Catal. A. 192 (2000) 181.
[9] C.T. Kresge, M.E. Leonowicz, W.J. Roth, J.C. Vartuli and J.S. Back, Nature 359 (1992) 710.
[10] D. Zhao, J. Feng, Q. Huo, N. Melosh, G.H. Fredrickson, B.F. Chmelka and G.D. Stucky, Science 279 (1998) 548.
[11] A. Corma, V. Fornes, M.T. Navarro and J. Perez-Pariente, J. Catal. 148 (1994) 569
[12] C.A. Koh, R. Nooney and S. Tahir, Catal. Lett. 47 (1997) 199
[13] S.T Wong, H.P Lin and C.Y. Mou, Appl. Catal. A. 198 (2000) 103.
[14] A. Sayari, Chem. Mater. 8 (1996) 1840.
[15] T. Lei, W.-M. Hua, Y. Tang, Y.-H. Yue and Z. Gao, J. Mol. Catal. A. 170 (2001) 195.
[16] Q.-H. Xia, K. Hidajat and S. Kawi, Chem. Commun. (2000) 2229.
[17] H. Matsuhashi, M. Tanaka, H. Nakamura and K. Arata, Appl. Catal. A. 208 (2001) 1.
[18] C.-L. Chen, H.-P. Lin, S.-T. Wong, S. Cheng and C.-Y. Mou, *Proceedings of the 3rd Seminar on Science and Technology Catalysis* (Fukuoka, Japan, 9–10 March 2000) p. 95.
[19] C.-L. Chen, S. Cheng, H.-P. Lin, S.-T. Wong and C.-Y. Mou, Appl. Catal. A. 215 (2001) 21.
[20] S. Wang and J.A. Guin, Energy and Fuels 15 (2001) 666.
[21] C.-L. Chen, T. Li, S. Cheng, H.-P. Lin, C.J. Bhongale, and C.-Y. Mou, Microporous Mesoporous Mater. (2001) in press.
[22] Z. Gao, Y. Xia, W. Hua and C. Miao, Topics Catal. 6 (1998) 101.
[23] W. Hua, Y. Xia, Y. Yue and Z. Gao, J. Catal. 196 (2000) 104.
[24] P. Canton, R. Olindo, F. Pinna, G. Strukul, P. Riello, M. Meneghetti, G. Cerrato, C. Morterra and A. Benedetti, Chem. Mater. 13 (2001) 1634.
[25] H.-P. Lin, S. Cheng and C.-Y. Mou, Microporous Mater. 10 (1997) 111.
[26] R.C. Garvie, J. Phys. Chem. 69 (1965) 1238.
[27] C. Morterra, G. Cerrato, F. Pinna and M. Signoretto, J. Catal. 157 (1995) 109.
[28] R.L. White, E.C. Sikabwe, M.A. Coelho and P.E. Resasco, J. Catal. 157 (1995) 755.
[29] M. Kruk, M. Jaroniec, C. H. Ko and R. Roo, Chem. Mater. 12 (2000) 1961.
[30] R. Roo, C.H. Ko, M. Kruk, V. Antochshuk and M. Jaroniec, J. Phys. Chem. B 104 (2000) 11465.
[31] M. Risch and E.E. Wolf, Appl. Catal. 206 (2001) 283.